

INSTALLATION OF METAL-BINDING FUNCTIONALITY AT LYSINE RESIDUES VIA AZIDE-ALKYNE
"CLICK CHEMISTRY"

by

Matthew Ryan Baucom

A Senior Honors Project Presented to the

Honors College

East Carolina University

In Partial Fulfillment of the

Requirements for

Graduation with Honors

by

Matthew Ryan Baucom

Greenville, NC

May 2015

Approved by:

William E. Allen, PhD

Chemistry Department

Thomas Harriot College of Arts and Sciences

ABSTRACT

A novel non-natural amino acid designed to bind divalent metal ions, dubbed Lys(PYRIT), was prepared in a “click reaction” by treating Fmoc-Lys(N₃)-OH with 2-ethynylpyridine and Cu(I). It was incorporated into a 12-residue peptide using standard Fmoc solid phase synthesis protocols. Multiple spectroscopic techniques (NMR, ESI-QToF-MS, UV-vis, and CD) confirm that the PYRIDINYL/Triazolyl side-chain binds Zn(II) and Cu(II) in the presence of competing natural residues such as histidine and glutamic acid. It remains unclear whether metal ions mediate the oligomerization of the Y2K PYRIT peptide, as is believed to be important in neurodegenerative diseases.

TABLE OF CONTENTS

LIST OF FIGURES	5
LIST OF TABLES	6
LIST OF SCHEMES	6
LIST OF ABBREVIATIONS	7
CHAPTER 1: INTRODUCTION	8
1.1 Alzheimer's and Significance of Neurodegenerative Diseases	8
1.2 Protein Aggregation and Metal Binding	12
1.3 Azide-Alkyne Click Chemistry	14
CHAPTER 2: SYNTHESIS OF FMOC-LYS(PYRIT)-OH AND Y2K PYRIT	15
2.1 Synthesis of FMOC-LYS(PYRIT)-OH via Azide-Alkyne Click Chemistry	15
2.2 Spectroscopic Properties of FMOC-LYS(PYRIT)-OH	17
2.3 Solid Phase Synthesis of Y2K PYRIT Peptide	19
2.4 On Resin Synthesis of FMOC-LYS(PYRIT)-OH	21
CHAPTER 3: Y2K PYRIT METAL BINDING STUDIES	23
3.1 Computational Studies	23
3.2 Nuclear Magnetic Resonance Studies	26

3.3 Mass Spectrometry Studies	28
3.4 UV-Vis Spectrometry Studies	30
3.5 Circular Dichroism Studies	33
CHAPTER 4: EXPERIMENTAL	37

LIST OF FIGURES

1.1 Structure of Amyloid Precursor Protein (APP)	9
1.2 Benign cleavage pathway of Amyloid Precursor Protein	10
1.3 Harmful cleavage pathway of Amyloid Precursor Protein	10
1.4 Plaque formation by amyloid-beta peptide	11
1.5 2,2-Bipyridine chelating a Zn(II) metal cation	13
1.6 1,3 dipolar cycloaddition of alkyne and azide producing only 1,4 regioisomer	14
2.1 Structure of pyridinyl-triazolyl functional group binding a Zn(II) metal cation	15
2.2 Mass spectra (ESI-QToF) of purified Fmoc-Lys(PYRIT)-OH	18
2.3 HPLC chromatogram of pure Fmoc-Lys(PYRIT)-OH detected at 300 nm	18
2.4 HPLC chromatogram of pure Fmoc-Lys(PYRIT)-OH detected at 214, 280, and 300 nm	19
2.5 Structure of Y2K PYRIT peptide shown with Lys(PYRIT) at residue 3	20
2.6 Mass spectrum of Y2K PYRIT	21
2.7 Mass spectrum of YYKEIAHALK(PYRIT)SA	22
3.1 Side by side comparison of two PYRIT functional groups binding a Cu(II) cation	24
3.2 DFT-optimized structure of helical K(PYRIT)EIAH	25
3.3 Aromatic region of the ¹ H-NMR spectrum of Y2K control	26

3.4 Aromatic region of the ^1H -NMR spectrum of Y2K(PYRIT) during Zn(II) titration	27
3.5 Mass spectra (ESI-QToF) of Y2K(PYRIT) during titration with $\text{Zn}(\text{BF}_4)_2$	29
3.6 Mass spectra (ESI-QToF) of Y2K(PYRIT) during titration with $\text{Cu}(\text{NO}_3)_2$	30
3.7 Electronic absorption spectra of Y2K(PYRIT) during titration with $\text{Cu}(\text{NO}_3)_2$	33
3.8 Far UV CD spectra displaying secondary structure characteristics	34
3.9 CD spectra of Y2K(PYRIT) and Y2K(PYRIT)-Cu	35

LIST OF TABLES

3.1 Titration of pyridine into a copper (II) nitrate solution	31
3.2 Titration of imidazole into a copper (II) nitrate solution	31
3.3 Titration of acetate into a copper (II) nitrate solution	31
4.1 Mass spectrometry parameters	40

LIST OF SCHEMES

2.1 Synthesis of Fmoc-Lys(PYRIT)-OH from FMOC-Lys-OH	16
--	----

LIST OF ABBREVIATIONS

AD - Alzheimer's disease

β A - Beta-Amyloid Peptide

ESI-MS – Electrospray Ionization - Mass Spectrometry

PYRIT – Pyridinyl Triazolyl functional group

Lys – Lysine

His – Histidine

Glu – Glutamic Acid

Tyr – Tyrosine

INTRODUCTION

1.1 Alzheimer's Disease and the Significance of Neurodegenerative Disorders

Alzheimer's disease (AD) is an irreversible neurodegenerative disorder that is the leading cause of dementia in those over the age of 65. This disease is characterized by the inability to perform simple tasks along with loss of cognitive functioning, memory, and reasoning. It also has a multiple negative effects on the behavior of those afflicted by the disorder. Currently it is estimated that between 2.4 and 4.5 million Americans suffer from AD, depending on the method of measurement.^{1,2} There are no known cures. However, recent studies have shown a slowing of progression in the presence of metal chelators, implicating transition metal ions like Cu(II) in the disease.

There are two types of AD, early- and late-onset. Early-onset Alzheimer's disease is much more rare and affects people between the ages of 30 and 60. Most cases of early-onset Alzheimer's are inherited, and are therefore known as familial AD (FAD).² Late-onset Alzheimer's disease is the more prevalent form that primarily affects those over the age of 65. The cause of Alzheimer's disease is not entirely clear but there have been arguments supporting genetic as well as environmental contributing factors.²

The genetic cause of Alzheimer's has been narrowed to a region of chromosome 19 where the gene coding for apolipoprotein E can be found. There are three alleles of the APOE protein including $\epsilon 2$, $\epsilon 3$, and $\epsilon 4$.² Those with the APOE $\epsilon 2$ allele are less likely to contract AD, or contract it later in life. The APOE $\epsilon 3$ allele has been shown to be neutral towards AD, while the APOE $\epsilon 4$ gene occurs in 40% of those with AD. This gene doesn't necessarily cause AD but there

is strong correlation between the APOE ϵ 4 allele and an increased risk of developing Alzheimer's disease.²

Although the cause remains unclear, the pathway for the formation of characteristic amyloid-beta plaques has been elucidated. Amyloid-beta ($A\beta$) plays a critical role in the mechanism of neurodegeneration and contributes to the development of AD through oxidative stress, mitochondrial dysfunction, impaired synaptic transmission, the disruption of membrane integrity, and impaired axonal transport.³ It has been found that the transmembrane amyloid precursor protein (APP) can undergo one of two processes during cleavage. Figure 1.1 below shows the normal structure of APP and the cleavage enzymes embedded in the neuronal membrane.

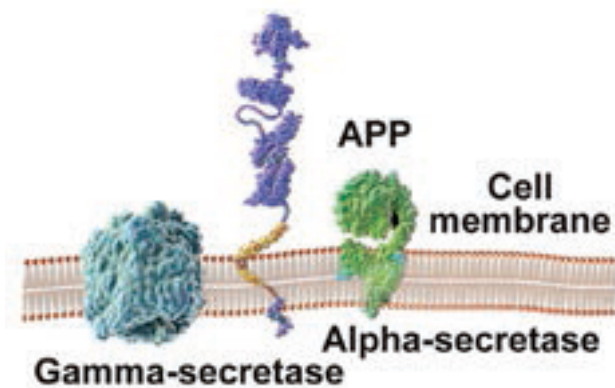


Figure 1.1: Structure of Amyloid Precursor Protein (APP) and cleavage enzymes in the neuronal membrane.²

In the normal benign pathway, the transmembrane protein APP is cleaved by alpha-secretase within the portion that would become the amyloid-beta protein. The cleaved portion of APP, sAPP α , has been found to promote neuronal growth and development.² The remaining

portion of APP is then cleaved a second time by gamma-secretase, releasing the remaining amyloid-beta portion outside of the cell and leaving the larger portion of APP inside the cell to interact with the nucleus to support growth (Figure 1.2).

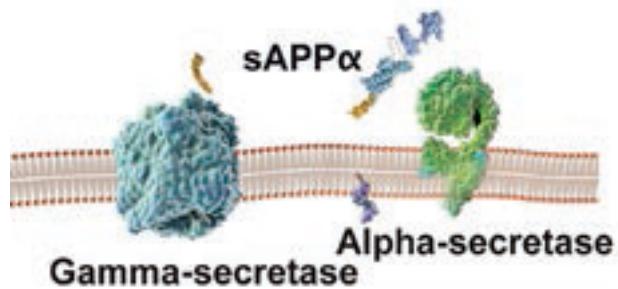


Figure 1.2: Benign cleavage pathway of Amyloid Precursor Protein.²

In the harmful APP cleavage pathway, beta-secretase cleaves the APP molecule at one end of the amyloid-beta peptide releasing sAPP β to the outside of the neuron. Gamma-secretase then cleaves the remaining APP molecule in its normal location at the other end of the amyloid-beta peptide.² This sequence of cleavages releases intact amyloid-beta peptide from the neuronal membrane to the cell's exterior (Figure 1.3).

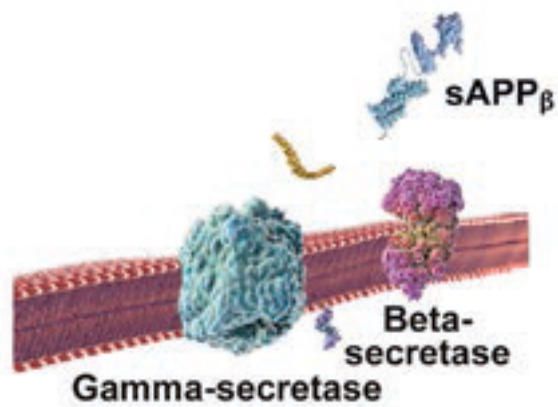


Figure 1.3: Harmful cleavage pathway of Amyloid Precursor Protein.²

The amyloid-beta ($A\beta$) peptides that are released from the neuronal membrane in the harmful cleavage pathway then begin to form oligomers, which are groups of two or more peptides aggregated together. These oligomers are thought to interact with specific synaptic connections between neurons, affecting neuronal communication.² As more $A\beta$ peptides group together, the oligomers form protofibrils and fibrils. The fibrils eventually group together with other cellular material and proteins to form insoluble plaques that are characteristic of AD.² A number of other neurodegenerative disorders, such as Parkinson's disease and Huntington's disease, are also caused by protein misfolding and aggregation.^{3,4}

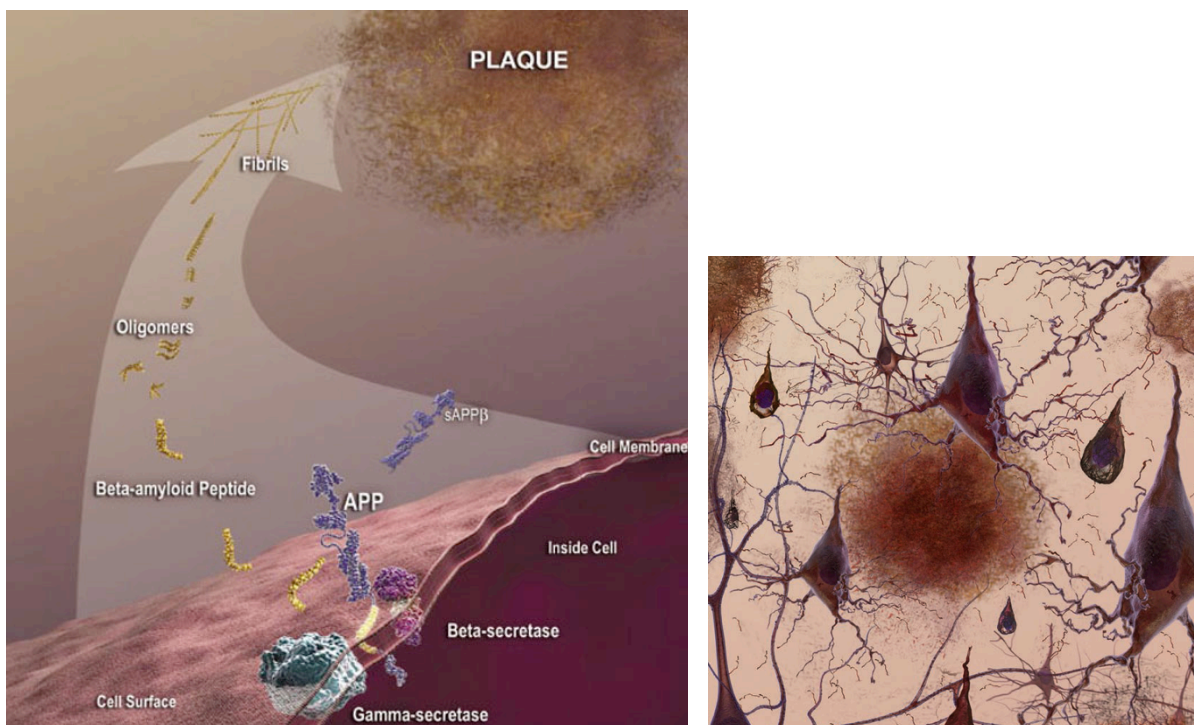


Figure 1.4: (a) Plaque formation by amyloid-beta peptide.² (b) Plaque disruption of neuronal communication and signaling.²

1.2 Protein Aggregation and Metal Binding

After amyloid-beta protein is released from the neuronal membrane it begins to form oligomers, which eventually lead to the development of insoluble plaques. Current research suggests that amyloid-beta binds metal cations such as Zn(II) or Cu(II) to facilitate oligomerization. Copper ions bind to soluble A β and precipitate them in slightly acidic solution (pH 6.6), while zinc ions bind to soluble A β and precipitate them over a wider range of pH (pH 5.5-7.5).³ Histidine residues within the amyloid-beta peptide play a critical role in metal binding. The nitrogen contained within the imidazole functional group donates a pair of electrons to the metal cations, acting as a monodentate ligand. A histidine residue at position 13 binds Zn(II) in human A β ₁₋₄₀ but is substituted for arginine in rat A β ₁₋₄₀. This histidine residue is crucial for the aggregation of A β --aggregation is reduced in rat peptides when compared to those of humans.^{4, 5} Histidine residues 6, 13, and 14 in the amyloid-beta peptide are responsible for binding Zn(II). In general, histidine is the amino acid most commonly involved in metal binding among the naturally occurring amino acids, but other residues such as glutamate, aspartate, and tryptophan may play a role in metal binding. Based on computational modeling, it has been found that histidine has a stronger binding affinity for Cu²⁺ than glutamate, aspartate, or tryptophan.⁶ Histidine was found to have a $\Delta G_{\text{binding}} = 374.9$ kcal/mol while glutamate was found to have a $\Delta G = 298.0$ with absolute values provided.⁶

Current research is being performed with Cu/Zn chelators to see if they can inhibit peptide aggregation. The drug Clioquinol, for example, has been shown to slow the progression of AD by dissolving plaques and preventing new oligomers from forming.⁷ Chelators operate by

essentially sequestering the metal ions, preventing them from binding amyloid-beta. One strong chelator that has been studied is the bidentate biheterocycle 2,2-bipyridine (bipy). The structure of bipy is shown below in Figure 1.5.

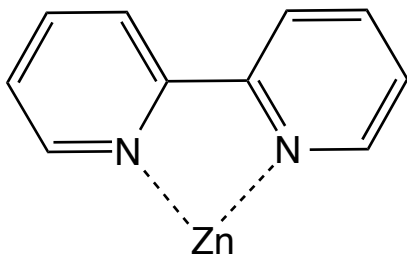


Figure 1.5: 2,2-Bipyridine chelating a Zn(II) metal cation.

Recent research has been directed toward adding bipy-like functional groups to the side chains of natural amino acids.^{8,9,10} Bipy fills two coordination sites on a metal ion, one from each nitrogen lone pair,¹⁰ allowing for strong peptide-metal binding with fewer residues than normally required to bind a metal cation. The bipy functional group has been incorporated onto alanine residues and has been shown to bind Zn^{2+} more efficiently than natural amino acids.¹⁰ A recent study by the Schultz group designed a genetically encoded bipyridylalanine amino acid.⁹ Another study synthesized a 1,2,3-triazole on the side chain of alanine to resemble the structure of histidine.⁸ By synthesizing new protected amino acids with a stronger affinity for metal ions, researchers have fuller control over the sites and stoichiometry of metal binding within a given peptide.

1.3 Amino Acid Azide-Alkyne Click Chemistry

“Click chemistry” is a term that was coined by Sharpless to describe reactions that have very high yields, no byproducts, and that almost invariably work.¹¹ The original and best-known click reaction, the Huisgen 1,3-dipolar cycloaddition between a terminal alkyne and an organic azide, can produce an undesired mixture of two triazole regioisomers (1,4 and 1,5). The groups of Meldal and later Sharpless showed that by using a copper(I) catalyst, only the 1,4 regioisomer is obtained.¹¹

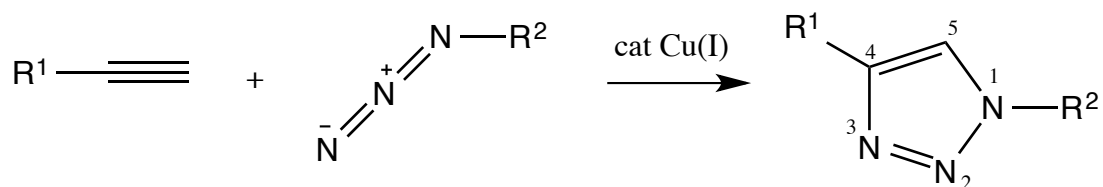


Figure 1.6: 1,3 dipolar cycloaddition of alkyne and azide producing only 1,4 regioisomer.

A few sources have reported performing click-chemistry reactions on Fmoc-protected amino azides.^{9,11,12} Some researchers have modified amino acids containing alcohols to become amino azides through Mitsunobu reactions.¹³ Most other peptidotriazoles prepared to date have incorporated the heterocycles within the peptide *backbone* or on one terminus of the peptide or the other. The following chapter will detail our efforts to incorporate pyridyl-triazoles into amino acid *side chains*.

CHAPTER 2: SYNTHESIS OF FMOC-LYS(PYRIT)-OH AND Y2K PYRIT

2.1 Synthesis of Fmoc-Lys(PYRIT)-OH via Azide-Alkyne Click Chemistry

The Crowley group at the University of Otago synthesized 2-pyridyl-1,2,3-triazole compounds via “click” chemistry and determined that they bind to metals very well.¹⁴ We reasoned that this reaction should yield 1,2,3-triazoles on the side chains of azide-bearing amino acid residues, allowing for incorporation of robust metal binding properties into peptides. Based on the high affinities for metals of 2,2-bipyridine and 2-pyridyl-1,2,3-triazole systems, the latter (Figure 2.1) should bind metal cations such as Cu(II) and Zn(II), provided they can “outcompete” naturally-occurring residues like His and Glu. The “PYRIT” name was chosen to highlight the presence of **PYR**idine and **Triazole** units, while emphasizing that this work was performed at East Carolina University, home of The Pirates.

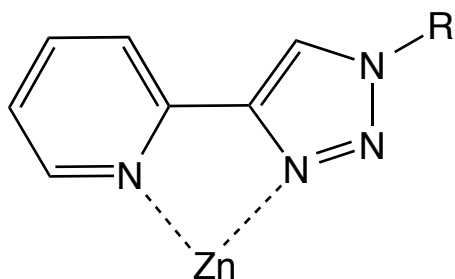
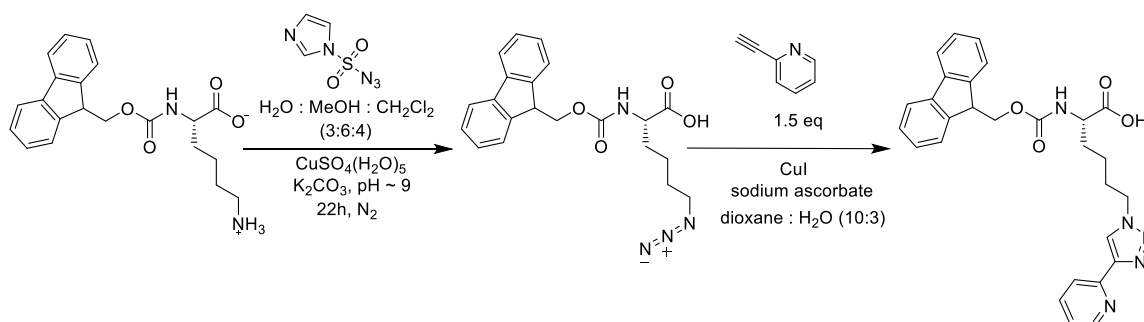


Figure 2.1: Structure of pyridinyl-triazolyl functional group binding to a Zn(II) metal cation.

To develop a general platform for installing metal binding functionality into any peptide, we decided to modify lysine residues. Lysine naturally contains a primary amino group that can be easily converted to an azide through use of an azide transfer agent like TMS-N₃.^{15,16} To our knowledge, no one has previously added a pyridinyl-triazolyl group to Lys. An azide could be

added to other natural amino acids, but initial addition of a primary amine to the terminus of the side-chain would require additional steps. Scheme 2.1 shows our approach to the addition of a pyridyl-triazolyl group to the side chain of lysine in two steps: an azide transfer reaction followed by a Huisgen 1,3-cycloaddition that forms a triazole.^{15,16,17}



Scheme 2.1: Synthesis of Fmoc-Lys(PYRIT)-OH from Fmoc-Lys-OH

Imidazole-1-sulfonyl azide hydrochloride was first prepared on a 3 gram scale in quantitative yield (Scheme 2.1).¹⁵ This azide transfer unit can be purchased but is easily synthesized in lab. Fmoc-Lys(N₃)-OH, while commercially available, is prohibitively expensive. It was therefore prepared using commercially available Fmoc-Lys-OH.¹⁶ The azide transfer reaction was performed in distilled water, methanol, and dichloromethane in a 3:6:4 (v:v:v) ratio. The reaction was catalyzed by copper(II) sulfate pentahydrate, and potassium carbonate was used to obtain a pH of 9, effectively deprotonating the primary amine. The reaction was performed under an inert atmosphere of nitrogen gas, and afforded a 98% yield of the Fmoc-Lys(N₃)-OH after 24 h of reaction time. The lysine-azide species was then incorporated into a Huisgen 1,3-cycloaddition reaction to generate Fmoc-Lys(PYRIT)-OH.¹⁷ This reaction was catalyzed by copper(I) iodide, in the presence of 1.5 equivalents of 2-ethynylpyridine, yielding approximately 15% of the desired product. Once the reaction was completed, the Fmoc-

Lys(PYRIT)-OH was purified through reversed-phase HPLC as a brown, sticky, resin-like compound. After lyophilization, tens of milligrams of the pure, dried amino acid could be obtained at a time as a brick-red solid.

2.2 Spectroscopic Properties of Fmoc-Lys(PYRIT)-OH

After synthesizing the novel amino acid Fmoc-Lys(PYRIT)-OH, HPLC on a C18 column was used for purification. Using gradient elution from 75% CH₃CN/25% H₂O to 25% CH₃CN /75% H₂O, the desired compound eluted at approximately 22 minutes. This separation was performed on a Vydac Protein and Peptide C18 prep scale column (22 x 250 mm, 20 μm) with a flow rate of 10.00 mL/min and detector set to 300 nm. The suspected peak was collected and mass spectrometry was used to determine the identity (Figure 2.2). The purified Fmoc-Lys(PYRIT)-OH was then subjected to HPLC again to confirm its purity, yielding one peak at 22 minutes (Figures 2.3 and 2.4). The UV-vis detector was set to detect at 214, 280, and 300 nm during these trials. Peptide bonds and many other biological molecules are detectable at 214 nm while tryptophan and tyrosine residues are detectable at 280 nm. The PYRIT functional group has strongest electronic absorption at 300 nm.

16-Feb-2015 Purified Fmoc-Lys-PYRIT-COOH
12:55:57
20150216_MRB_FMOCLYS_PYRIT 42 (0.779) Cm (3.51)

TOF MS ES+
2.78e5

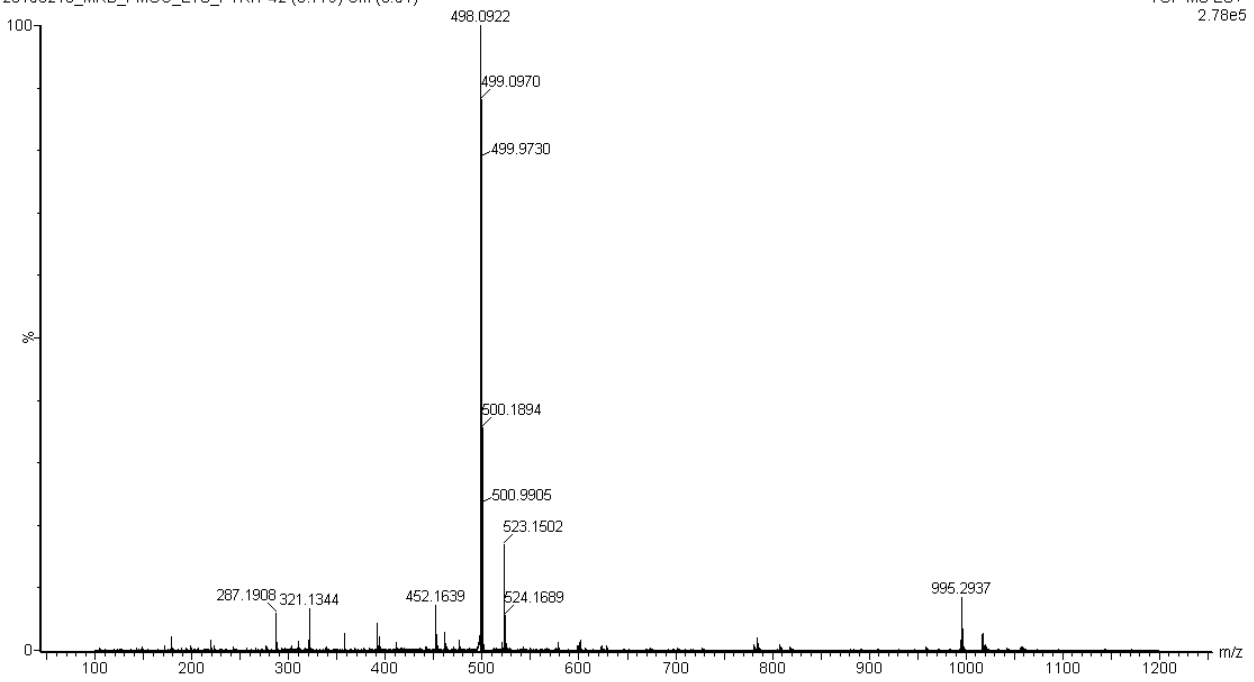


Figure 2.2: Mass spectra (ESI-QToF) of purified Fmoc-Lys(PYRIT)-OH ($[M+H]^+ = 498.2136$).

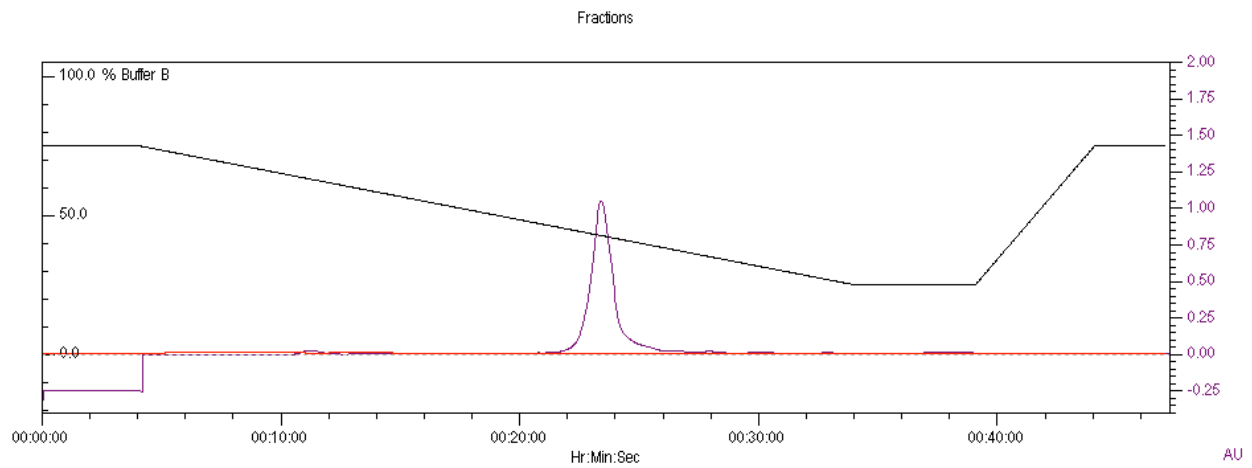


Figure 2.3: HPLC chromatogram of pure Fmoc-Lys(PYRIT)-OH detected at 300 nm.

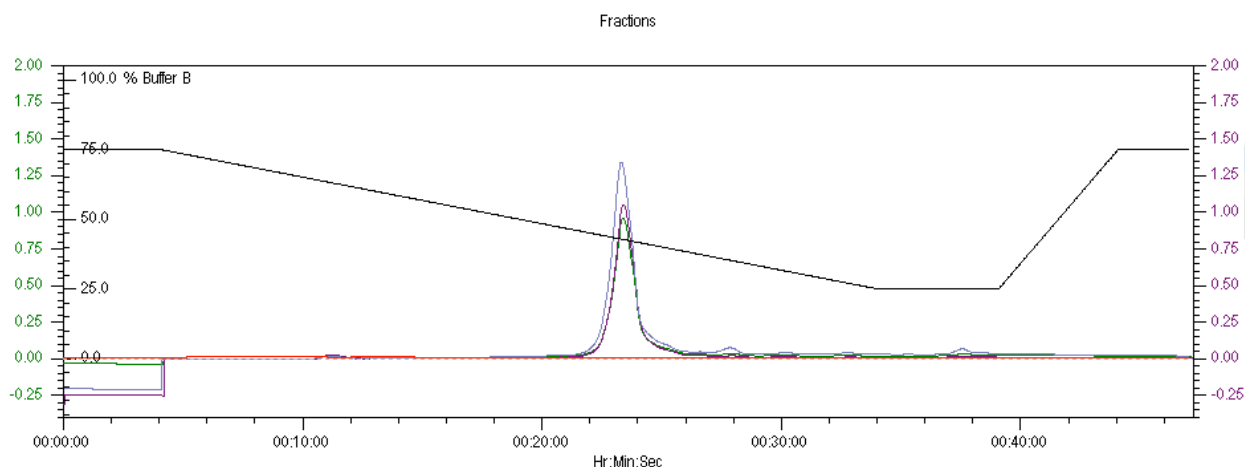


Figure 2.4: HPLC chromatogram of pure Fmoc-Lys(PYRIT)-OH detected at 214, 280, and 300 nm.

2.3 Solid Phase Synthesis of Y2K PYRIT Peptide

With approximately 55 mg of the purified Fmoc-Lys(PYRIT)-OH in hand, we wished to confirm if it could be used in standard automated peptide synthesis. It was thus incorporated into a 12-residue peptide, the sequence of which was derived from a recent publication from the DeGrado group.¹⁸ These researchers from the University of California at San Francisco developed an alpha-helical peptide called “Rocker” which was shown to form tetramers within a lipid bilayer; the tetrameric assembly is capable of transporting zinc ions across the membrane. The 12-residue sequence containing the zinc-binding site was taken from the N-terminus of 24-residue “Rocker:”

Rocker: **YYKEIAHALFSALFALSELYIAVRY**

A majority of the residues in Rocker are hydrophobic, as it was designed to localize in membranes. To ensure water-solubility of our 12-mer for various studies, the second Tyr residue was substituted with Lys, to give control peptide “Y2K:”



Finally, Lys(PYRIT) was installed at the second lysine (position 3 in the sequence) The Lys(PYRIT) was inserted here because it was expected to be close enough to the His at position 7 to allow for a metal ion to form a bridge between both residues. (The Rocker peptide binds zinc between the Glu at residue 4 and the His at residue 7.)



The 12-residue Y2K and Y2K(PYRIT) were synthesized using standard solid phase synthesis protocols and then cleaved off of the resin. Its identity was confirmed by ESI-MS (Figure 2.6).

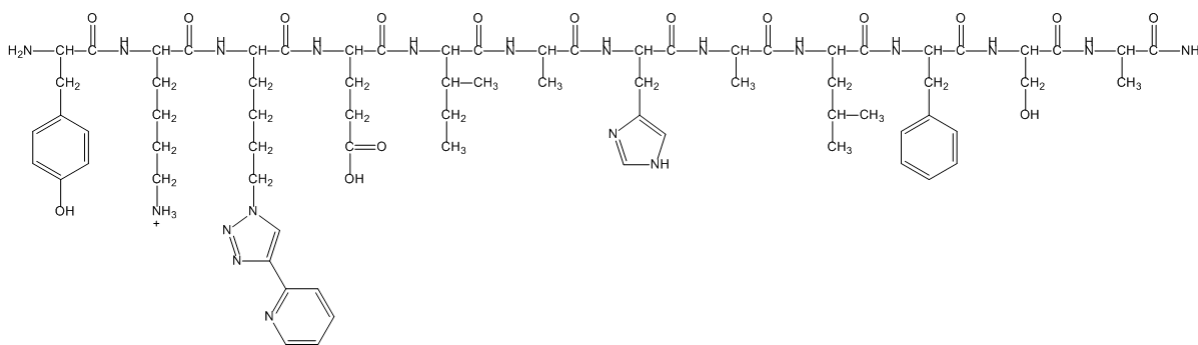


Figure 2.5: Structure of Y2K PYRIT peptide shown with Lys(PYRIT) at residue 3.

16-Mar-2015 Acetonitrile/water Y2KK* with no Cu added
09:37:22
031615_MRB_Y2KK_B 1 (0.025)

TOF MS ES+
2.94e3

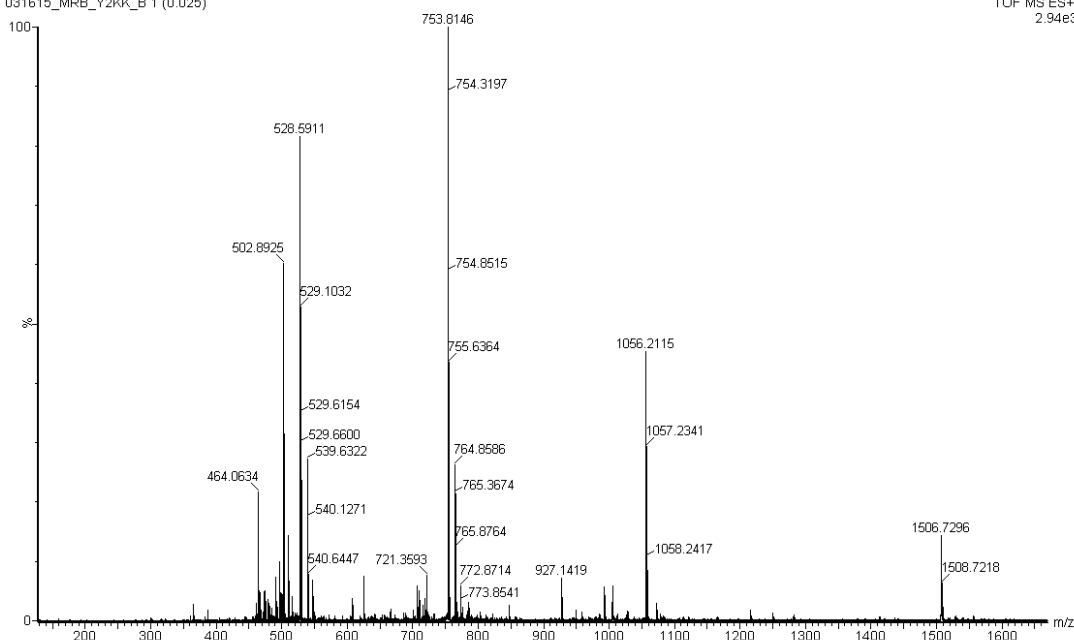


Figure 2.6: Mass spectrum of Y2K PYRIT showing $[M+H]^+ = 1505.8012$ and $[M+2H]^{2+} = 753.4042$.

2.4 On Resin Synthesis of Fmoc-LYS(PYRIT)-OH

An on-resin synthesis of a peptide 12-mer containing a Lys(PYRIT) residue was attempted, to determine whether the “click reaction” could be performed by the automated synthesizer. At the outset, it was unknown whether the triazole-forming reaction would tolerate DMF solvent and the presence of other functional groups from the resin and peptide strand. The reaction vessel of the peptide synthesizer was first loaded with Rink Amide resin and copper(I) iodide. Fmoc-Lys(azide)-OH was loaded into a vial at the desired Lys(PYRIT) position. The next vial in the sequence contained 2-ethynyl pyridine and sodium ascorbate.

After the Lys(azide) was incorporated into the peptide, the 2-ethynylpyridine and sodium ascorbate were dissolved with DMF in the usual manner, and upon automated transfer to the reaction vessel, a color change suggested a reaction was occurring. The crude peptide so obtained was purified via HPLC to yield YYKEIAHALK(PYRIT)SA, which was confirmed through ESI-MS with an m/z of 1521.7961. Synthesis of the Fmoc-Lys(azide)-OH is not required as it is commercially available. By performing the “click” reaction on resin, the synthesis and incorporation of Lys(PYRIT) is widely available to biochemists and other no-organic chemists if a protein synthesizer is available.

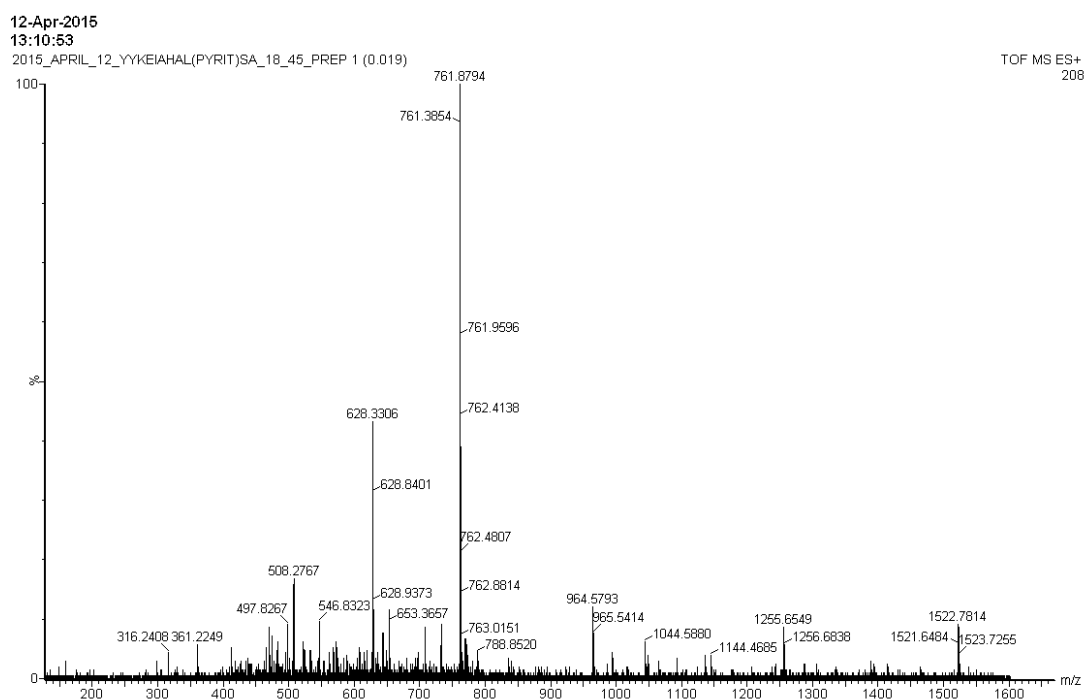


Figure 2.7 Mass spectrum of YYKEIAHALK(PYRIT)SA showing $[M+H]^+ = 1521.7961$ and $[M+2H]^{2+} = 761.4017$.

CHAPTER 3: Y2K PYRIT METAL BINDING STUDIES

3.1 Computational Studies

Computational studies were performed to determine whether the PYRIT functional group would bind zinc and copper ions, and more specifically, if two PYRIT functional groups, on the same peptide, could coordinate a single copper(II) in a square planar geometry. According to DFT analyses, if the two PYRIT functional groups approach the metal cation in a head to head fashion (Figure 3.1), the binding would not be stable due to steric hindrance. In contrast, if the two PYRIT groups bound the metal cation in a head-to-tail fashion, the dihedral angle is lowered and the binding is possible. This led to the conclusion that if two PYRIT groups were to bind one metal ion, the two residues would have to be far enough apart in the peptide to form a hairpin loop, or would have to be part of two separate peptides.

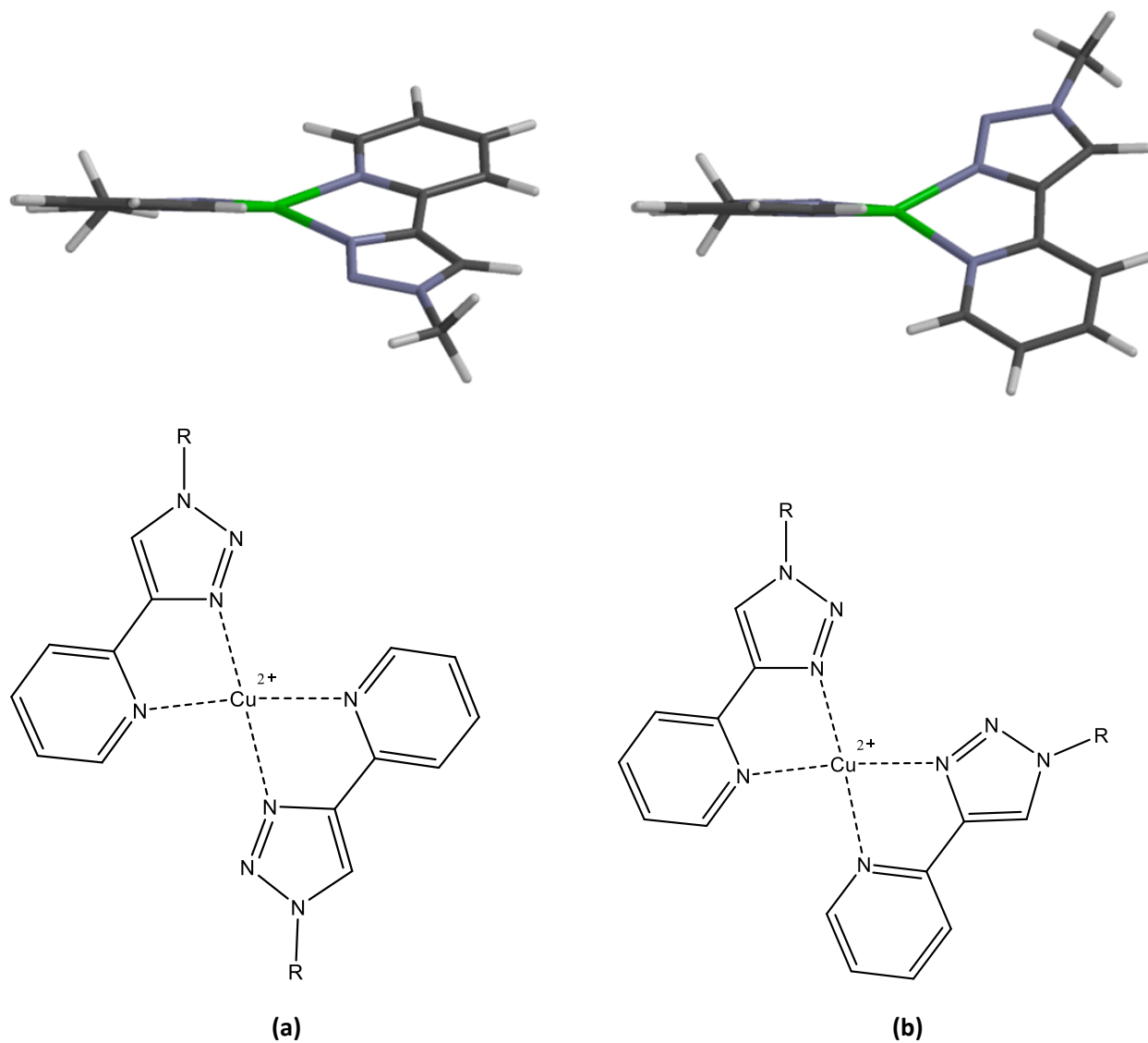


Figure 3.1: Side by side comparison showing (a) head to tail orientation (29.9° dihedral angle) and (b) head to head orientation (43.7° dihedral angle) of two PYRIT functional groups binding a Cu(II) cation.

Further computational analysis was performed after the 12-mer was identified as the targeted peptide. A five-residue sequence from the Y2K PYRIT peptide was selected for modeling. This sequence began with PYRIT at the N-terminus and went to Histidine at the C-terminus, therefore the sequence was K(PYRIT)EIAH. It was first modeled in a solvent continuum corresponding to water to determine if the suspected alpha helical secondary structure would be favored. The structure was determined to be stable in an alpha helical structure and more studies are being conducted to determine if the helix is conserved after metal binding between the PYRIT residue and the His residue.

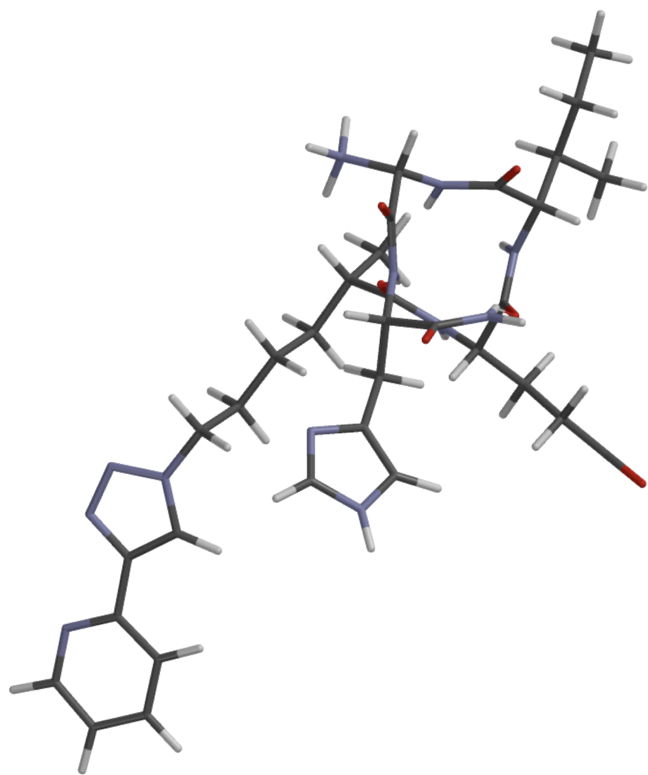


Figure 3.2: DFT-optimized structure of helical K(PYRIT)EIAH in a solvent continuum corresponding to water.

3.2 Nuclear Magnetic Resonance Studies

Proton NMR studies were performed in D_2O to determine which of the residues in Y2K PYRIT were binding to the metal cations. These studies were conducted by titrating in Zn(II). Copper was unable to be tested using NMR because of its paramagnetic properties. A proton NMR spectrum was first acquired for the pure Y2K peptide to determine the chemical shifts of the PYRIT peaks. Figure 3.3 shows the aromatic region of the Y2K control peptide while Figure 3.4 shows the aromatic region of Y2K PYRIT.

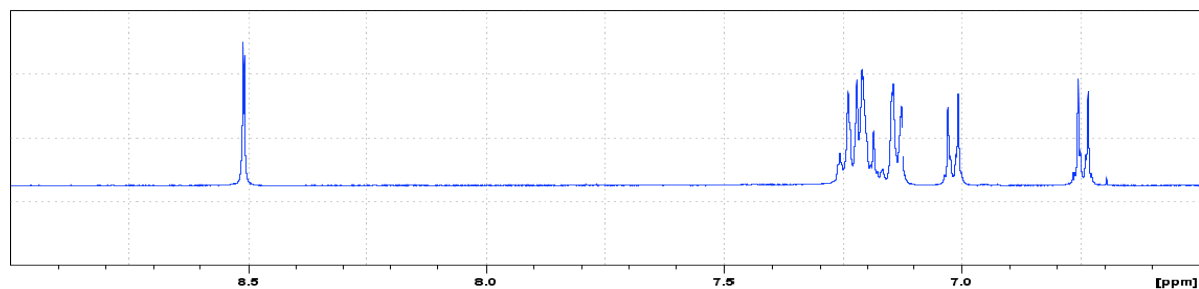


Figure 3.3: Aromatic region of the 1H -NMR spectrum of Y2K control in D_2O .

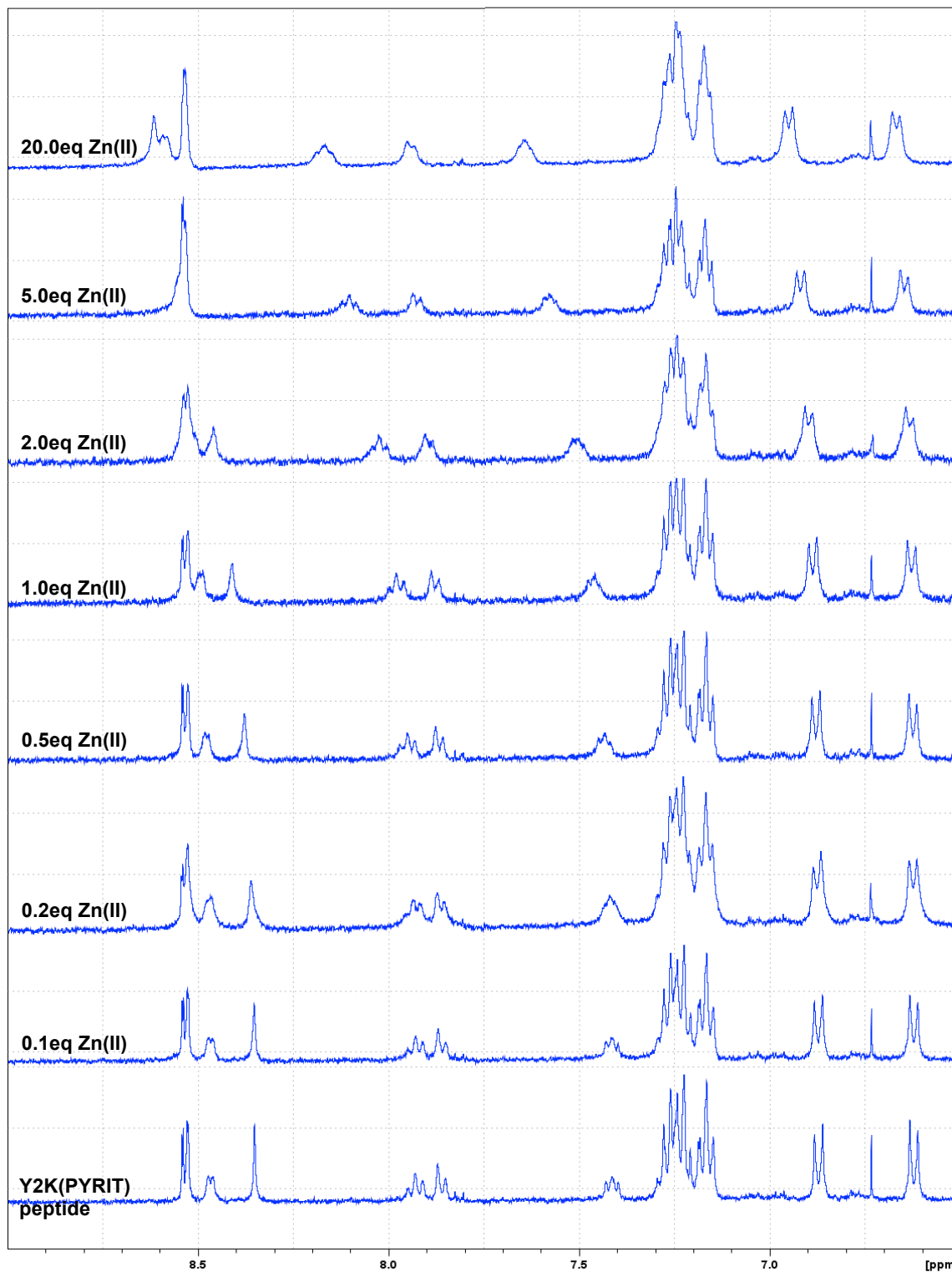


Figure 3.4: Aromatic region of the ^1H -NMR spectrum of Y2K(PYRIT) during titration with $\text{Zn}(\text{BF}_4)_2$ in D_2O .

After inspection of the proton NMR spectra of Y2K and Y2K PYRIT, it was determined that the peaks corresponding to the PYRIT unit appear at the following chemical shift values: 7.42, 7.87, 7.93, 8.35, and 8.46 ppm. These peaks are present in the Y2K PYRIT spectrum but are not present for control Y2K. Each of these peaks shifts downfield as more zinc is titrated into the Y2K PYRIT solution. After 20.0 eq of Zn(II) has been added, the aromatic protons exhibit chemical shift values of 7.65, 7.95, 8.17, 8.58, and 8.62 ppm, respectively. This is consistent with the zinc ion binding the PYRIT functional group, deshielding the surrounding protons.

3.3 Mass Spectrometry Studies

The Y2K PYRIT peptide was further analyzed using mass spectrometry while titrating in Zn(II) in the form of $\text{Zn}(\text{BF}_4)_2$. As shown in Figure 3.5, both free Y2K PYRIT and zinc-bound Y2K PYRIT were initially present before adding any zinc. This suggests that PYRIT is such an effective metal binder that it was able to bind adventitious metal ions found in the glassware, solvent, or within the mass spectrometry instrument. As more Zn(II) was introduced, the Y2K PYRIT-Zn peak increased in intensity, while a separate Y2K PYRIT-Zn- BF_4 peak developed and grew rapidly in size. This shows that the peptide was binding the zinc metal as well as binding one of the tetrafluoroborate counterions.

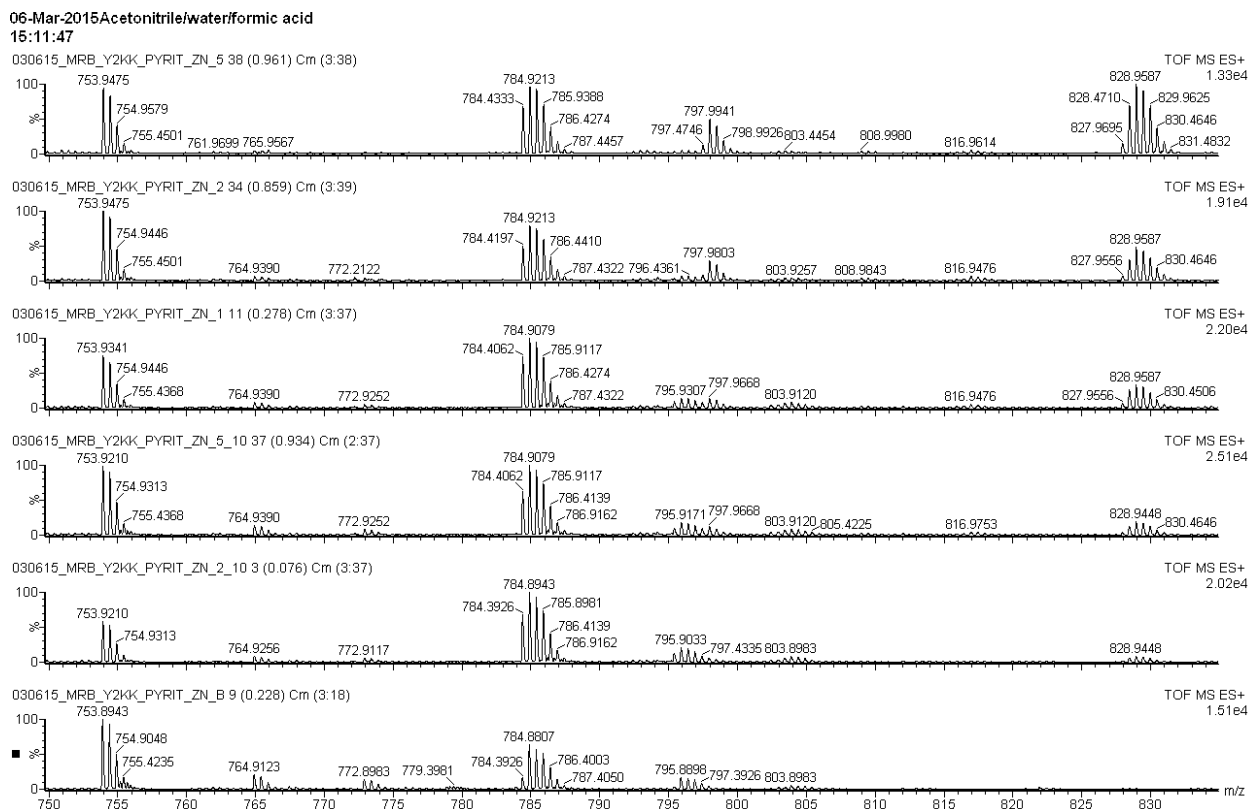


Figure 3.5: Mass spectra (ESI-QToF) of Y2K(PYRIT) during titration with $Zn(BF_4)_2$.

A mass spectrometry study was also completed using copper cations. The Y2K PYRIT peptide was first analyzed without adding in any Cu(II) ($[M+2H]^{2+} = 753.8126$). Aliquots of aqueous copper(II) nitrate were then added to achieve Cu(II) stoichiometries of 0.1, 0.2, 0.5, 1.0, 2.0, and 5.0 relative to peptide. As shown in Figure 3.6 the initial sample contained no peptide bound to copper. As the Cu(II) was titrated in, the Y2K PYRIT-Cu peak ($[M+2H]^{2+} = 784.3383$) continued intensifying until after 5.0 eq were present, at which point there was no unbound Y2K PYRIT left. This shows that all of the peptide in solution was bound to copper cations and suggests that the PYRIT functional group is a very effective copper-binding moiety.

16-Mar-2015 Acetonitrile/water Y2KK* with no Cu added
09:37:22

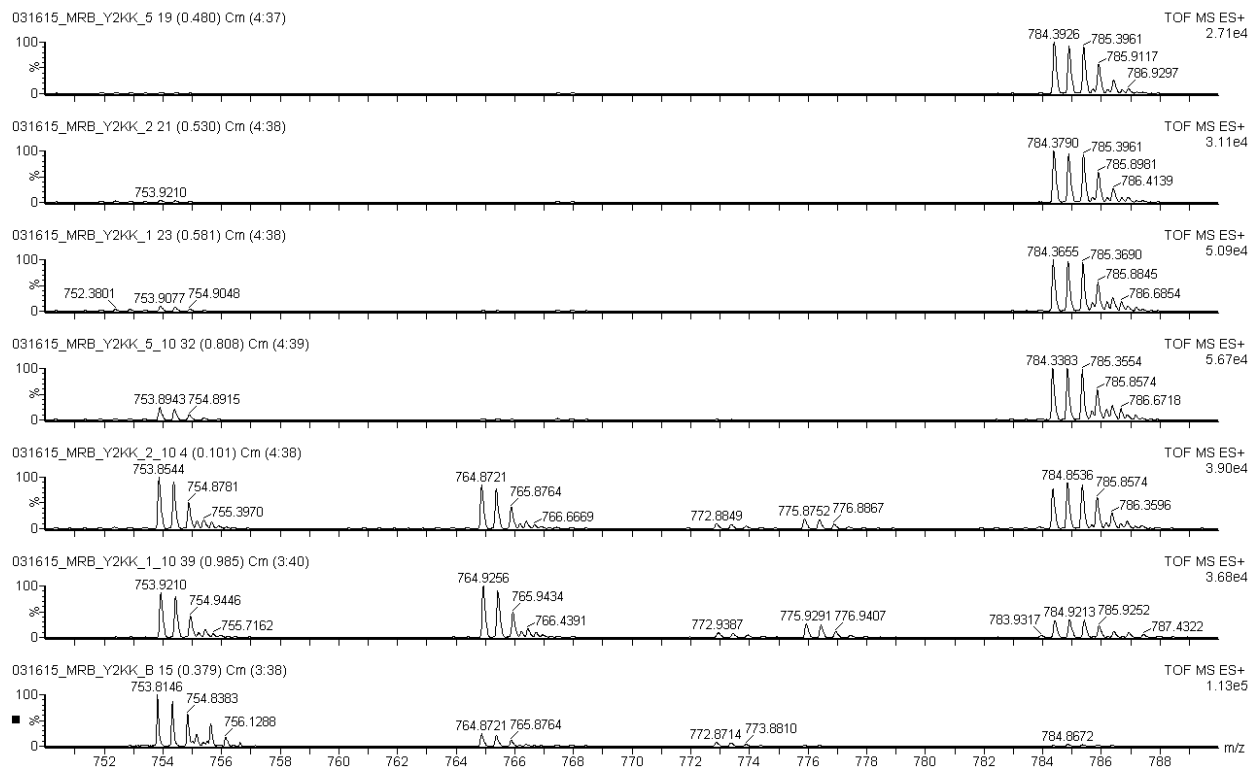


Figure 3.6: Mass spectra (ESI-QToF) of Y2K(PYRIT) during titration with $\text{Cu}(\text{NO}_3)_2$.

3.4 UV-Vis Spectrometry Studies

The Y2K PYRIT peptide was analyzed using UV-Vis spectroscopy to determine which residues in the sequence have the greatest affinity for copper. Before performing the UV-Vis analysis of Y2K PYRIT, absorption spectra were obtained for copper(II) complexes of the simple ligands pyridine, imidazole, and acetate as shown in Tables 3.1, 3.2, and 3.3, respectively. Here, solutions of the ligands were transferred into aqueous $\text{Cu}(\text{NO}_3)_2$ in a cuvette while following the shift in the absorption maximum. It was observed that pyridine shifts to a λ_{max} of approximately 648 nm when saturated with Cu(II). Imidazole yields an absorption maximum of

approximately 592 nm when saturated with Cu(II), while acetate only shifts to approximately 761 nm.

Volume (μL)	λ_{\max} (nm)	Abs.	Eq.
1	796	0.19253	0.1
2	782	0.21421	0.2
5	753	0.26093	0.5
10	721	0.33540	1.0
20	682	0.46239	2.0
40	648	0.62975	4.0

Table 3.1: Titration of 7 M pyridine into a 22.4 mM Cu(NO₃)₂ solution showing a shift in λ_{\max} to approximately 648 nm when fully saturated.

Volume (μL)	λ_{\max} (nm)	Abs.	Eq.
1	780	0.19484	0.1
2	765	0.22973	0.2
5	729	0.28957	0.5
10	684	0.40951	1.0
20	617	0.59593	2.0
40	592	0.72260	4.0

Table 3.2: Titration of 7 M Imidazole into a 22.4 mM Cu(NO₃)₂ solution showing a shift in λ_{\max} to approximately 592 nm when fully saturated.

Volume (μL)	λ_{\max} (nm)	Abs.	Eq.
2	799	0.19252	0.1
4	792	0.21423	0.2
10	780	0.25195	0.5
20	773	0.30112	1.0
40	765	0.35362	2.0
80	761	0.39811	4.0

Table 3.3: Titration of 3.5 M sodium acetate into a 23.8 mM Cu(NO₃)₂ solution showing a shift in λ_{\max} to approximately 761 nm when fully saturated.

A 0.196 M copper(II) nitrate solution was prepared and titrated into a 1.07 μ M Y2K PYRIT peptide solution while measuring absorbance. The peptide solution concentration was obtained by first measuring the absorbance at 279 nm, 1.2827 AU. Using Beer's Law and the extinction coefficient for tyrosine at 280 nm (1200 AU/mMole/mL), the concentration was predicted to be 1.07 μ M. This means that 4.83 mg of Y2K PYRIT was dissolved in 3 mL of deionized water. As shown in Figure 3.7 below, initially there was no absorbance in the range of 500 – 900 nm. After the addition of 0.5 eq of $\text{Cu}(\text{NO}_3)_2$ there was an initial absorbance increase around 643 nm. This increase was maintained until 2.0 eq were present, and at 3.0 eq of Cu(II) an increase at 774 nm was observed. Based on the reference absorbance maxima obtained, we conclude that the Y2K PYRIT initially binds Cu(II) at the PYRIT functional group. Pyridine, which is most similar to the PYRIT moiety, exhibited an absorbance maxima of approximately 648 nm when saturated with Cu(II), while imidazole and acetate had absorbance maxima of 592 and 761 nm, respectively. Since 643 nm is close to 648 nm, the initial Cu(II) binding is suspected to be occurring at the PYRIT functional group. Once 3.0 eq of the Cu(II) cation is added, the absorbance maximum occurs around 774 nm. Thus, once there are 3.0 eq present, binding takes place at the glutamic acid residue. The peptide may still be binding metal at PYRIT but the absorbance maxima is covered up by the larger peak at 774 nm. Although binding does occur at the Glu residue, it is preferred at PYRIT at lower concentrations of Cu(II), suggesting that the binding is highly favorable.

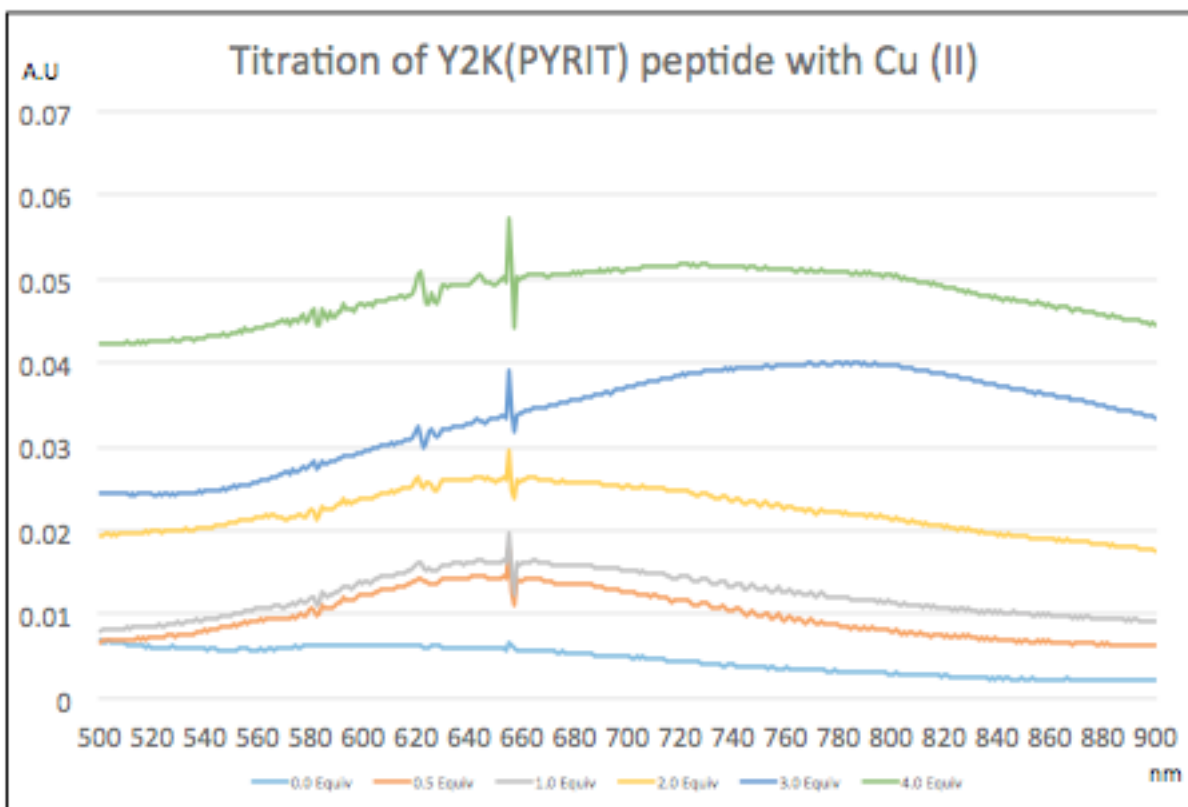


Figure 3.7: Electronic absorption spectra of Y2K(PYRIT) during titration with $\text{Cu}(\text{NO}_3)_2$. $\lambda_{\text{max}} = 643 \text{ nm}$ at 0.5 eq Cu (orange); 1.0 eq (grey), and 2.0 eq (yellow); $\lambda_{\text{max}} = 774 \text{ nm}$ at 3.0 eq (dark blue) and 4.0 eq (green).

3.5 Circular Dichroism Studies

Circular dichroism was utilized to study the secondary structure of Y2K PYRIT. The peptide was first analyzed without adding any metal, and then approximately 4 eq of $\text{Cu}(\text{NO}_3)_2$ was added and another spectrum was acquired. As shown in Figure 3.8, alpha-helical CD spectra tend to show two minima between 200 and 230 nm while β -sheet shows one minimum in that region. Random coils show a minimum at approximately 195 nm.¹⁹

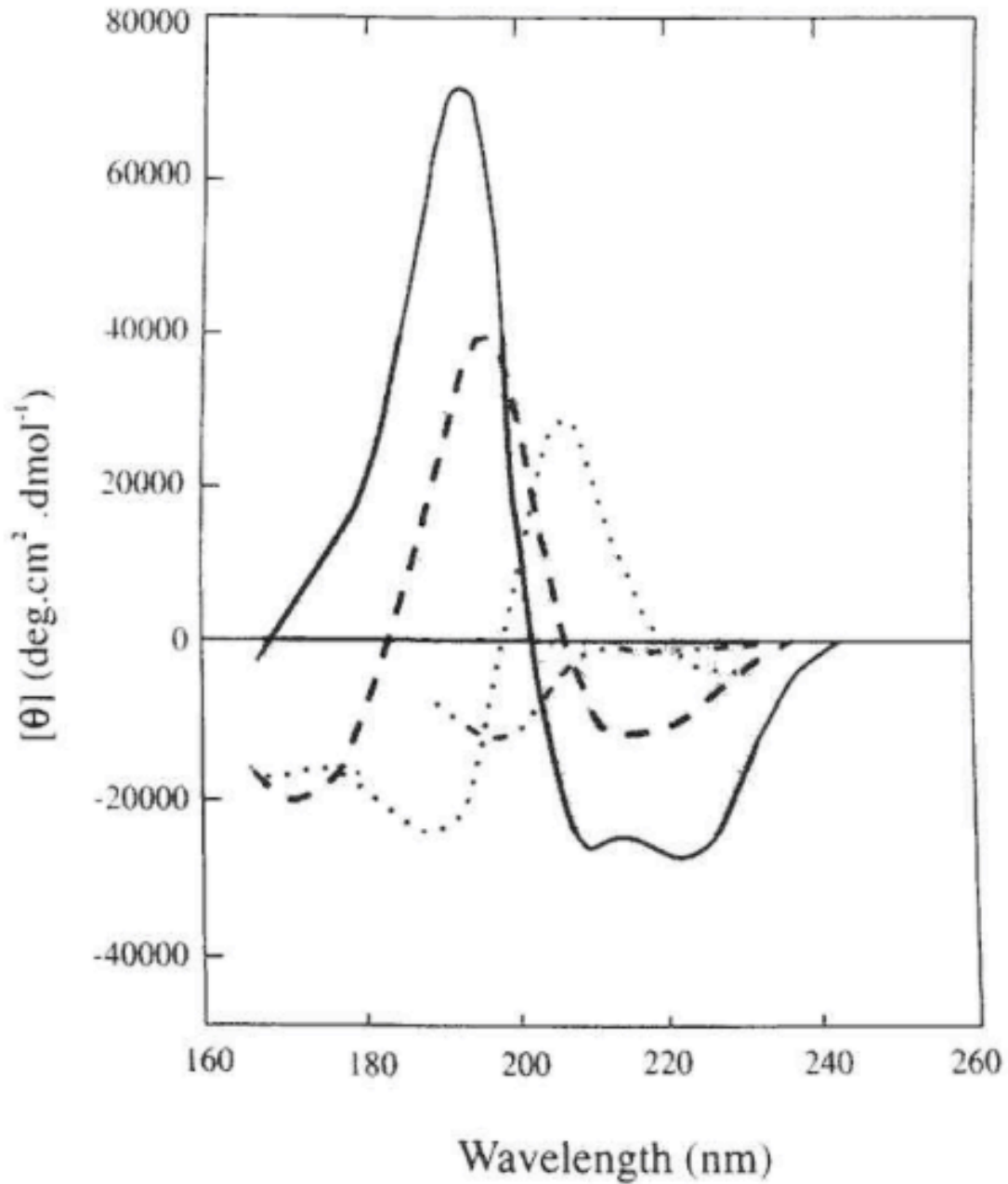


Figure 3.8: Far UV CD spectra displaying secondary structure characteristics. α -helix, solid curve; antiparallel β -sheet, long dashes; type I β -turn, dots; and random coil, short dashes.¹⁹

Based on the spectra obtained, a random coil orientation is suspected. This is not surprising; peptide sequences of fewer than 20 residues, like that found in the Y2K PYRIT

molecule, are typically unstructured.²⁰ Furthermore, because the CD study was performed in pH 7.4 phosphate buffer and not in a nonpolar solvent, hydrogen-bonds that might stabilize a helix are weakened. This solvent system was chosen to simulate physiological conditions, however the Rocker peptide from which Y2K PYRIT is based was designed to incorporate into cellular membranes. Therefore the CD study needs to be repeated using propanol, octanol, and/or liposomes to determine if the suspected alpha helical secondary structure is observed in a more nonpolar environment.

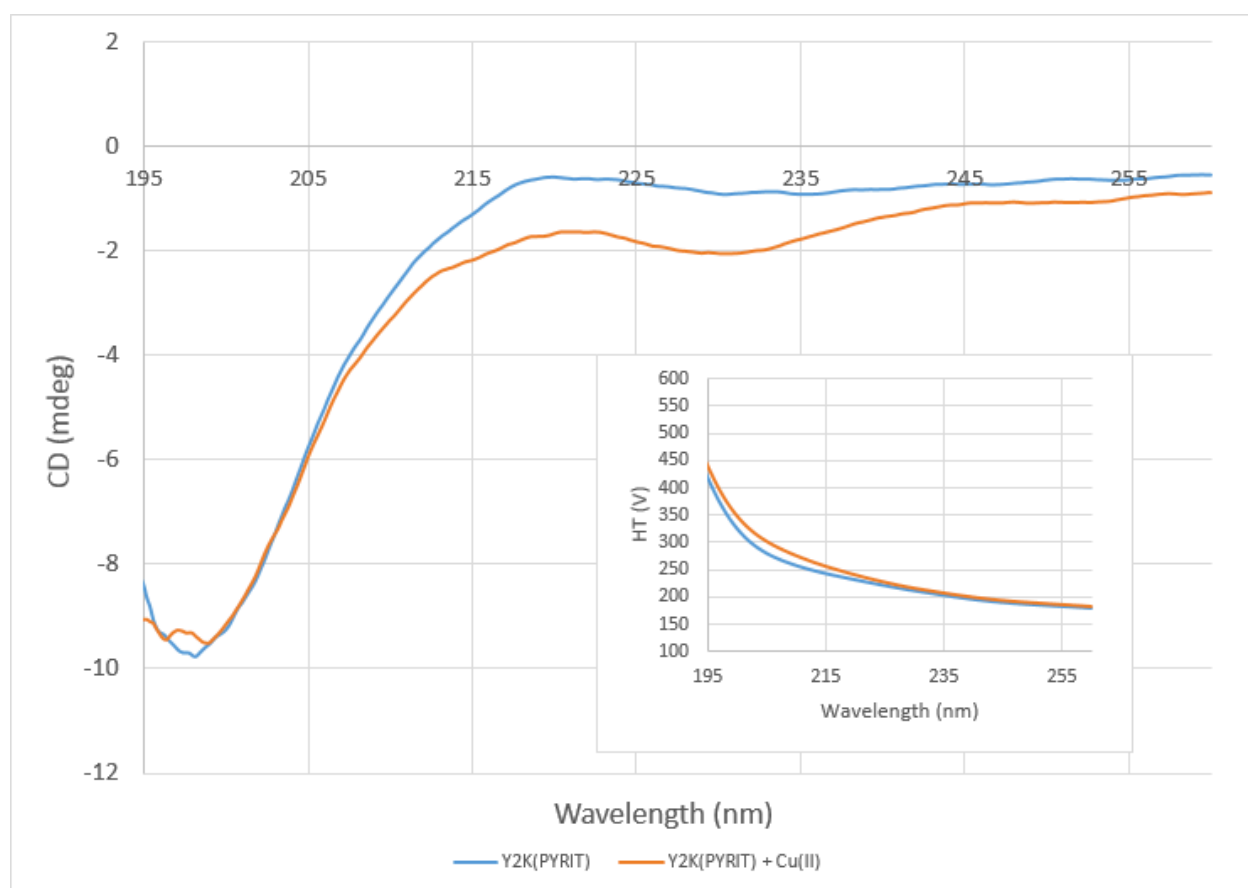


Figure 3.9: CD spectra of Y2K(PYRIT) and Y2K(PYRIT)-Cu showing random coil-like secondary structure in pH 7.4 phosphate buffer solution.

Conclusions

Lys(PYRIT) has been shown to be an effective metal chelator that can be incorporated into peptides through two routes: Solution-phase synthesis of Fmoc-Lys(PYRIT)-OH followed by standard solid phase peptide synthesis, or click chemistry upon a resin-bound Fmoc-Lys(N₃). This novel amino acid has been shown to bind Cu²⁺ and Zn²⁺ efficiently via UV-Vis, NMR, and ESI-MS. Future work will be focused on running azide transfer and click reactions upon full peptides with native lysine residues already present. If successful, the PYRIT side-chain could find broad use as a means to add metal-binding functionality at sites where it otherwise wouldn't be. Circular dichroism studies will also be repeated using propanol, octanol, or liposomes to simulate a nonpolar cellular membrane. It is expected that Y2K PYRIT should assume an alpha helical secondary structure in this environment.

EXPERIMENTAL

Synthesis of Fmoc-Lys(N₃)-OH:^{15,16} Commercially available Fmoc-Lys-OH (1.14 g, 3.10 mmol) was suspended in 40 mL of CH₂Cl₂ / 20 mL H₂O / 10 mL EtOH, and 1.95 g (9.30 mmol) of azido-transfer reagent was added. CuSO₄•5H₂O (8.0 mg, 0.05 mmol) was introduced, and the pH was increased from 2 to approximately 8-9 with aq. K₂CO₃. The resultant biphasic suspension was light blue in color and slightly opaque. The reaction was allowed to run for 20 hours before acidifying using 10% aq. HCl to pH of 6. The mixture was transferred to a separatory funnel and diluted with 75 mL CH₂Cl₂. The organic layer was washed with brine and dried over Na₂SO₄, before being filtered. The faintly blue filtrate was then rotovapped and a partially viscous blue liquid was obtained and dried under vacuum for 40 minutes. The crude yield was 1.26 g. This material was dissolved in 100 mL of CH₂Cl₂ and washed with 10% HCl then brine before being dried over Na₂SO₄. After filtration and evaporation, the faintly gold oil was dried under vacuum to afford 1.20 g (3.08 mmol, 98%) of Fmoc-Lys(N₃)-OH.

Synthesis of Fmoc-Lys(PYRIT)-OH:¹⁷ Freshly prepared Fmoc-Lys(N₃)-OH (564 mg, 1.43 mmol) was dissolved in 35 mL of dioxane and 15 mL of deionized water. Approximately 1.5 eq of 2-ethynylpyridine (221 mg) was added to the solution along with CuI (14.8 mg) and sodium ascorbate (18.1 mg). The clear, dark yellow solution was allowed to stir at room temperature for 18 h, during which time the color became dark purple. The solvents were removed by rotary evaporation and 50 mL of CH₂Cl₂ was added to the dried product. The solution was washed three times in a separatory funnel with 10 mL of 10% HCl. Copper precipitated out of solution during the acid wash. The organic layer was isolated and dried over Na₂SO₄. The liquid was

then filtered and the filtrate evaporated under reduced pressure. Approximately 600 mg of a solid, gel-like brown product was obtained and further purified via reversed-phase HPLC. HPLC was performed using a Vydac Protein and Peptide C18 prep scale column (22 x 250 mm, 20 μ m) at a flow rate of 10.00 mL/min and a linear gradient from 25% CH₂Cl₂ / 75% H₂O to 75% CH₂Cl₂ / 25% H₂O over 30 minutes while detecting at 300 nm. The Fmoc-Lys(PYRIT)-OH eluted at 16.5 minutes and was then lyophilized. After lyophilization, 55 mg of product was obtained providing a 2.5% yield after purification. The identity of the product was confirmed using ESI-QToF-MS (*m/z* calcd for [M+H]⁺ 498.2136; found 498.0922).

An on-resin azide-alkyne “click” reaction. Synthesis of YYKEIAHALK(PYRIT)SA-CONH₂: The reaction vessel of an automated peptide synthesizer programmed for standard Fmoc solid-phase protocols was charged with 339 mg of Rink Amide MBHA resin (loading 0.59 mmol/g, 0.20 mmol) and 12.0 mg of CuI. Vials containing the appropriate Fmoc-protected amino acids and HBTU (0.60 mmol of each) were set into the carousel. Duplicate vials were prepared to allow for double coupling of residues Y1, Y2, L9, K(N₃)10, and A12. The PYRIT-functionalized side-chain of residue 10 was constructed *in situ* by first appending Fmoc-Lys(N₃)-OH to the growing strand in the usual manner. Upon advancing to the next vial, the synthesizer dissolved the contents (2-ethynylpyridine (62 mg) and sodium ascorbate (20 mg)) in DMF, and transferred the alkyne solution to the reaction vessel. After 90 minutes, with periodic agitation of the resin and Cu(I) salt provided only by automated nitrogen bubbling, the synthesizer deprotected the newly-formed Fmoc-Lys(PYRIT) residue and completed the remainder of the synthesis. The resin was removed from the reaction vessel, rinsed with glacial CH₃COOH, CH₂Cl₂, and finally CH₃OH, and dried under high vacuum for 2 h. The peptide was cleaved from

the resin by treatment with a mixture of TFA/TIS/anisole/water for 1 h, and was precipitated by addition of ice-cold diethyl ether. The crude material so obtained (175 mg) was purified by preparative-scale RP-HPLC on a C18 column (22 x 250 mm, 20 μ m), using a linear gradient of 100% water to 100% CH₃CN at a flow rate of 10 mL/min over 30 minutes. Four peaks that absorbed at 300 nm were observed, at retention times of 13:30, 17:55, 18:45, and 21:00. The second of these was found to be an 11-mer lacking Y, but the third peak proved to be the desired 12-mer by ESI-QToF mass spectrometry (m/z calcd for [M + H]⁺ 1521.7961, found 1521.7620; calcd for [M + 2H]²⁺ 761.4017, found 761.3987). The eluate was lyophilized to a white powder.

Studies of metal binding by proton NMR were completed using a Bruker 400 MHz instrument over 256 scans each. Y2K PYRIT (2.3 mg) was dissolved in 1.00 mL D₂O and a spectrum was acquired with no metal added. Zinc(II) tetrafluoroborate (370 mg) was dissolved in 10.00 mL of D₂O and then titrated into the NMR tube containing the peptide sample. After each addition of Zn(II), a spectrum was acquired and proton shifts were observed. It was found that the proton signals corresponding to the PYRIT protons shifted downfield with the addition of Zn(II).

Mass spectra were acquired on a Micromass Q-ToF Micro mass spectrometer with electrospray ionization source. The samples were dissolved in 1:1 acetonitrile/water solutions and spectra were obtained over a 100 – 3200 m/z range. Parameters used during ESI-MS analysis are listed in Table 4.1 below.

Ion Mode	ES +
Flow Rate	10 μ L/min
Source Temperature	80°C
Desolvation Temperature	120°C
Capillary Voltage	2500 V
Sample Cone	30 V
Extraction Cone	2.0 V
Cone	20 L/hr
Desolvation	500 L/hr

Table 4.1: Mass spectrometry parameters.

Absorption spectra were obtained using an Agilent Cary 8454 UV-Vis. The spectra were acquired from 190 nm to 850 nm using a 3.0 mL quartz cuvette with path length 1 cm.0

CD studies were performed using pH 7.4 phosphate buffer and 1.0 mm quartz cuvettes. The spectra were obtained from 190 to 350 nm and the HT values were kept below 450 V.

References

1. National Institute on Aging. Fact Sheet. 2011. NIH Pub. No. 11-6423
2. Alzheimer's Disease: Unrevealing the Mystery, National Institute on Aging. 2008. NIH Pub. No. 08-3782
3. Crouch, P.; Harding, S.; White, A. Camakaris, J.; Bush, A.; Masters, C. Mechanisms of AB mediated neurodegeneration in Alzheimer's Disease. *Int. J. Biochem. Cell B.* **2008**, *40*, 181-198
4. Adlard, P.; Bush, A. Metals and Alzheimer's Disease. *J. Alzheimers Dis.* **2006**, *10*, 145-163.
5. Bush, A. The metallobiology of Alzheimer's Disease. *Trends Neurosci.* **2003**, *26*, 207-214.
6. Jover, J.; Bosque, R.; Sales, J. A comparison of the binding affinity of the common amino acids with different metal cations. *Dalton Trans.* **2008**, 6441-6453.
7. Cherny, A.; Atwood, C.; Xilinas, M.; Gray, D.; Jones, W.; McLean, C.; Barnham, K.; Volitakis, I.; Fraser, F.; Kim, Y.; Huang, X.; Goldstein, L.; Moir, R.; Lim, J.; Beyreuther, K.; Zheng, H.; Tanzi, R.; Masters, C.; Bush, A. Treatment with a Copper-Zinc Chelator Markedly and Rapidly Inhibits B-Amyloid Accumulation in Alzheimer's Disease in Transgenic Mice. *Neuron.* **2001**, *30*, 665-676.

8. Nadler, A.; Hain, C.; Diederichsen, U. Histidine Analog Amino Acids Providing Metal-Binding Sites Derived from Bioinorganic Model Systems. *Eur. J. Org. Chem.* **2009**, 4593-4599.
9. Xie, J.; Liu W.; Schultz, P. A Genetically Encoded Bidentate, Metal-Binding Amino Acid. *Angew. Chem.* **2007**, *119*, 9399-9402.
10. Cheng, R.; Fisher, S.; Imperiali, B. Metallopeptide Design: Tuning the Metal Cation Affinities with Unnatural Amino Acids and Peptide Secondary Structure. *J. Am. Chem. Soc.* **1996**, *118*, 11349-11356.
11. Angell, Y.; Burgess, K. Peptidomimetics via copper-catalyzed azide-alkyne cycloadditions. *Chem. Soc. Rev.* **2007**, *36*, 1674-1689.
12. Moses, J.; Moorhouse, A. The growing applications of click chemistry. *Chem. Soc. Rev.* **2007**, *36*, 1249-1262.
13. Tornøe, C.; Christensen, C.; Meldal, M. Peptidotriazoles on Solid Phase: [1,2,3]-Triazoles by Regiospecific Copper(I)-Catalyzed 1,3-Dipolar Cycloadditions of Terminal Alkynes to Azides. *J. Org. Chem.* **2002**, *67*, 3057-3064.
14. Lo, W.; Huff, G.; Cubanski, J.; Kennedy, A.; McAdam, C.; McMorran, D.; Gordan, K.; Crowley, J. Comparison of Inverse and Regular 2-Pyridyl-1,2,3-triazole "Click" Complexes: Structures, Stability, Electrochemical, and Photophysical Properties. *Inorg. Chem.* **2015**, *54*, 1572-1587.
15. Goddard-Borger, E.; Stick, R. *Org. Lett.* **2007**, *9*, 3797-3800.

16. Lau, Y.; Spring, D.; *Syn. Lett.* **2011**, *13*, 1917-1919.
17. Feldman, A.; Colasson, B.; Fokin, V. *Org. Lett.* **2004**, *6*, 3897-3899.
18. Joh, N.; Wang, T.; Bhate, M.; Acharya, R.; Wu, Y.; Grabe, M.; Hong, M.; Grigo, G.; DeGrado, W.; *Science.* **2014**, *346*, 1520-1524.
19. Kelly, S.; Price, N. The Use of Circular Dichroism in the Investigation of Protein Structure and Function. *Curr. Protein Pept. Sc.* **2000**, *1*, 349-384.
20. Scholtz, J.; Baldwin, R. The Mechanism of α -helix Formation by Peptides. *Annu. Rev. Biophys. Biomol. Struct.* **1992**, *21*, 95-118.